Review

Peng Shi, Luping Du* and Xiaocong Yuan*

Spin photonics: from transverse spin to photonic skyrmions

https://doi.org/10.1515/nanoph-2021-0046
Received February 3, 2021; accepted October 7, 2021;
published online October 21, 2021

Abstract: Spin angular momentum associated with circular polarization is a fundamental and important aspect of photons both in classical and quantum optics. The interaction of this optical spin with matter and structures results in many intriguing optical effects and state-of-the-art applications covered under the emerging subject of spin optics. Distinct from longitudinal optical spin along the mean wavevector, transverse spin, the corresponding vector of which is perpendicular to the mean wavevector, prevails and plays a significant role in confined electromagnetic waves such as focused beams, guided waves, and evanescent waves. In the optical near-field, these transverse spins are generated owing to the spatial variation of the kinetic momentum of confined electromagnetic waves, where the spin and orbital angular momenta are strongly coupled, leading to many interesting topological spin structures and properties. Several reviews on optical transverse spins have been published in recent years in which their concepts and the various configurations producing them were introduced systematically. Here, we introduce in this review the underlying physics and dynamics of transverse spin and the resultant topological structures and properties such as the photonic skyrmions and merons. We term this sub-area 'spin photonics', its scope being to cover the design and research of spin structures in strongly confined electromagnetic fields with unique properties and applications. The concepts and framework reviewed have importance in optics, topological photonics, metrology, and quantum technologies and may be used to extend spin-dynamics concepts to fluidic, acoustic, and gravitational waves.

Keywords: angular momentum; spin-momentum locking; spin-orbit interaction; topological structure; transverse spin.

1 Introduction

In the classical physics, light is an electromagnetic (EM) wave, which has multiple degrees of freedom including frequency, amplitude, phase, and polarization [1, 2]. After 1900s, it is widely accepted that light has the wave-particle duality, which indicates a photon can be regarded as a particle containing the degrees of freedom including momentum and angular momentum (AM) [3–15]. The seminal work by Poynting in 1909 [3] demonstrated that the momentum carried by a photon is associated with its direction of propagation ($\mathbf{p} = \hbar\sigma\mathbf{k}$), being proportional to the local wavevector $\mathbf{k}$. Besides momentum, light beams also carry multiple kinds of angular momenta [4–15]. Generally, the AM of an optical beam is classed as: (i) intrinsic orbital AM (*i*-OAM) $\mathbf{L}_{\text{int}}$ [4–15] related to the optical phase singularity, which is characterized by the vortex topological charge; (ii) extrinsic orbital AM (*e*-OAM) $\mathbf{L}_{\text{ext}}$ [16, 17] associated with the beam trajectory, which depends on the transverse coordinates of the beam centroid; and (iii) spin AM (SAM) [18–24] associated with the rotation of electric and magnetic polarizations. Therein, the right- and left-handed circularly polarized plane waves, corresponding to EM helicity $\sigma = \pm1$, can be regarded as two spin states of a photon [19, 20]. Owing to the transversality of the EM wave ($\mathbf{k}\bullet\mathbf{E} = 0$), these spin vectors of right- and left-handed circularly polarized plane waves that are parallel to the direction of propagation of light (evaluated by the local wavevector $\mathbf{k}$) [19–22] and are considered as the longitudinal-type optical spin (*l*-SAM, $\mathbf{S}_l$).

The investigation of the interplay and mutual conversion between these types of optical AMs is covered under the topic spin–orbit interaction (SOI) of light (Figure 1; sections in green). First, the interaction between *l*-SAM and *e*-OAM

***Corresponding authors: Luping Du and Xiaocong Yuan**, Nanophotonics Research Center, Shenzhen Key Laboratory of Micro-Scale Optical Information Technology and Institute of Microscale Optoelectronics, Shenzhen University, Shenzhen 518060, China, E-mail: lpdu@szu.edu.cn (L. Du), xcyuan@szu.edu.cn (X. Yuan). https://orcid.org/0000-0003-2605-9003 (X. Yuan)
Peng Shi, Nanophotonics Research Center, Shenzhen Key Laboratory of Micro-Scale Optical Information Technology and Institute of Microscale Optoelectronics, Shenzhen University, Shenzhen 518060, China. https://orcid.org/0000-0001-9583-9412

results in a family of effects concerning helicity-dependent trajectories or momenta of light, including the spin Hall effect [25–38], the optical Magnus effect [16, 17, 39], the Coriolis effect [40, 41], and the plasmon Aharonov–Bohm effect [42]. Correspondingly, the orbit–orbit coupling between the *i*-OAM and *e*-OAM results in a vortex-dependent shift of light, which can be regarded as an orbital-Hall effect [43–45]. Additionally, the coupling between *l*-SAM and *i*-OAM produces intense spin-to-orbital AM conversions [46–49].

Besides the longitudinal-type optical spin discovered and demonstrated near a century ago [18], scientists in recent years found the existence of transverse-type optical spin (*t*-SAM, $\mathbf{S}_t$) for which the spin vector is perpendicular to the propagating direction of the optical field [19–22, 50–61]. This transverse optical spin is a fundamental AM property of light prevailing in confined EM waves [19–22], even for the single polarized confined modes [50–57], generated through the inhomogeneity of EM field and determined by the spatial structure of the kinetic

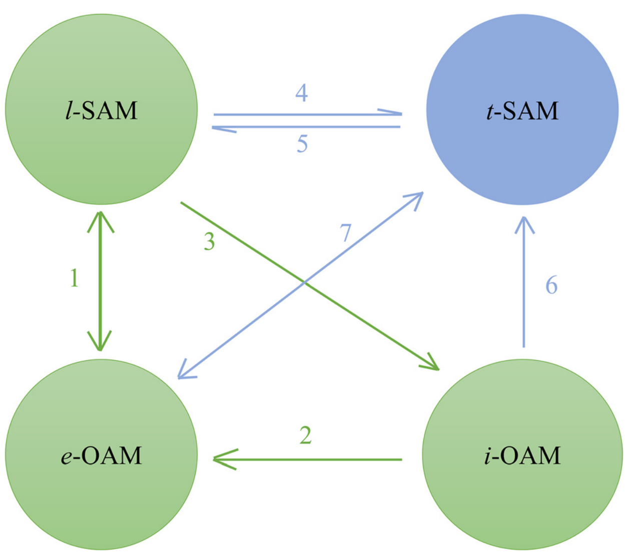

Figure 1: Various intriguing optical effects resulted from the interplay and mutual conversions between different types of AMs. ① Optical spin Hall effect [25–38]; ② orbital Hall effect [43–45]; ③ spin-to-orbital AM conversions [46–49]; ④ spin-controlled unidirectional emission [62–66, 88–94]; ⑤ the inversed effect of ④ [62]; ⑥ orbital-to-spin AM conversion [54, 55, 70–74]; ⑦ spin momentum locking and quantum spin Hall effect of light [57, 58, 67–69]. Noteworthily, no matter whether the spin-controlled unidirectional emission or its inverted effect, they can be decomposed into two processes. For example, the spin-controlled unidirectional emission in Ref. [79] includes the processes: (1) the *l*-SAM couples with the *t*-SAM and (2) the *t*-SAM excites the unidirectional light due to the property of spin-momentum locking. Vice versa, the inverted effect of spin-controlled unidirectional emission in Ref. [62] includes the processes: (1) the directional light excite the *t*-SAM due to the property of spin-momentum locking and (2) the *t*-SAM couples to the determined *l*-SAM.

momentum density [57]. Remarkably, the interplay between *t*-SAM and the other types of AMs underlies the many fascinating optical phenomena, extending the prospects for SOI applications of light (Figure 1; section in blue). For example, the coupling between the *t*-SAM and longitudinal spin results in a helicity-dependent unidirectional scattering or excitation of guided modes (Figure 2b), and vice versa (Figure 2c) [62–66]. This behavior arises from the intrinsic spin–momentum locking associated with evanescent waves which is considered the photonic counterpart of the quantum spin Hall effect (Figure 2a) [57, 58, 67–69]. In contrast, the coupling between *i*-OAM and *t*-SAM prompts an orbital-to-spin AM conversion, which occurs widely in focusing and scattering configurations [54, 55, 70–74]. Interestingly, this orbital-to-spin AM conversion would not produce additional net helix, which indicate that this spin is helix-free and consistent with the extraordinary properties of *t*-SAMs of the single polarized modes (helix-free, integral vanishing, and irrelated to geometric phase). Remarkably, considering spin–orbit coupling in optical vortices of evanescent waves, photonic-type spin skyrmions [75–82] (Figure 2d), which possess chiral spin texture similar to quasi-particles in magnetic materials in condense matter physics, were discovered. They attract widespread interest in the field of spin and topological photonics and have potential applications in directional scattering and transportation of photons [62–66, 83], nanometrology [84–87], chiral quantum optics [88–94], optical manipulation and communications [95–99], and spin-based robust optical surfaces [57, 67–69].

In the last few years, several reviews have been published that systematically introduce the concept of optical transverse spin and the various configurations in which it can be produced [19–22]. In this review, we focus on introducing the underlying physics and dynamics of transverse spin and the resultant topological structures. We start with a theoretical classification and description of the multiple dynamical properties of light, followed by a discussion of the dynamical generation of transverse spin and its relationship to the various recently discovered topological structures and their associated properties. Finally, we overview the current experimental techniques that characterize the optical transverse spin, and end with a discussion of this new area and its prospects.

2 Energy, momentum and angular momentum of light

To evaluate the *t*-SAM and its topological origin analytically and quantitatively, we first introduce the fundamental

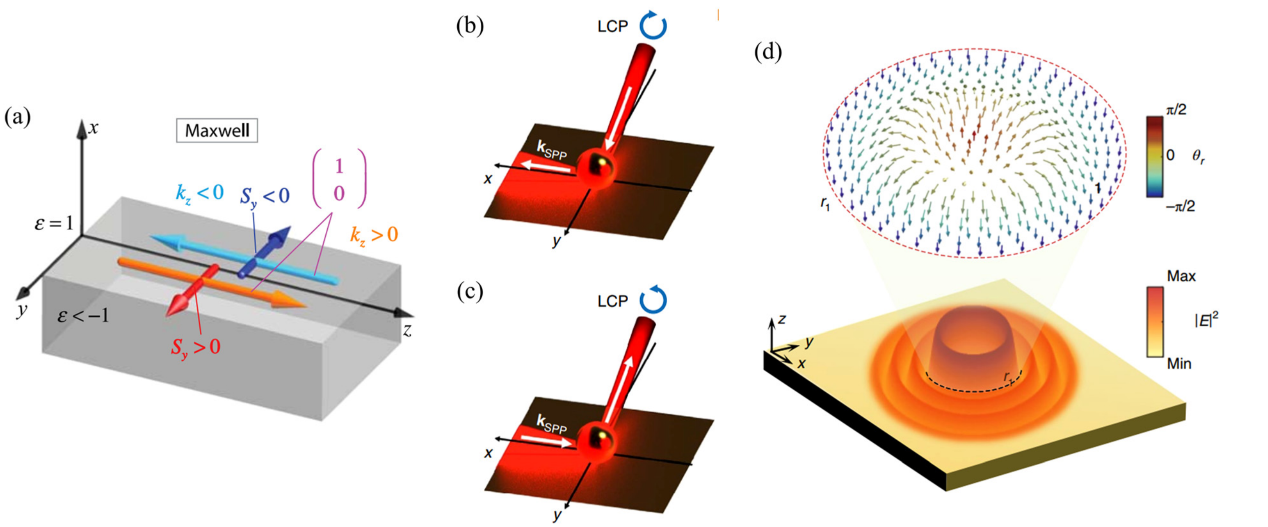

Figure 2: Optical phenomena associated with transverse spin: (a) optical analog of the quantum spin-Hall effect in a single polarized evanescent plane wave, for which the transverse spin vector is strictly locked to the direction of momentum [67]; (b) helix-controlled unidirectional emission of surface mode arising from the spin–momentum locking of *t*-SAM [62]; (c) the inversed effect of (b): direction-dependent excitation of helical modes [62]; and (d) photonic spin skyrmion formed in a single polarized evanescent optical vortex through spin–orbit coupling [75].

dynamical quantities in describing the optical momentum and the SAM. Although these dynamical properties of light have been studied thoroughly in several existing reviews [19–22], we still exhibit the relevant results for the convenience of explaining the origin, spin-momentum locking and topological properties of Maxwell surface fields from the spin and momentum points of view. For a time-harmonic monochromatic EM wave (**E**: electric field; **H**: magnetic field) with angular frequency ω in a lossless and passive homogeneous medium with permittivity ε and permeability μ, the time-averaged energy density (W) can be expressed as [1, 2]

$$W = \frac{1}{4}\left\{\epsilon|\mathbf{E}|^2 + \mu|\mathbf{H}|^2\right\} = \langle\psi|\psi\rangle, \tag{1}$$

where the 6-vector $|\psi\rangle = [\sqrt{\epsilon}\,\mathbf{E}, i\sqrt{\mu}\,\mathbf{H}]^{\mathrm{T}}/2$ represents the photon wave function [100–109] and superscript T signifies the transpose of the matrix. Here, the SI units are used through the manuscript. Noteworthily, only the measurable physical quantities at the air half space are considered here and thus we ignore the dispersion in the paper [110–112]. The kinetic momentum density **p** of the EM field in free space can be described by the Poynting vector **P** as [1–3, 100, 113]

$$\mathbf{p} = \mathbf{P}/c^2 = \frac{1}{2c^2}\mathrm{Re}\{\mathbf{E}^* \times \mathbf{H}\} = \langle\psi|\hat{\boldsymbol{\tau}}/c|\psi\rangle = \langle\hat{\boldsymbol{\tau}}/c\rangle, \tag{2}$$

Where the symbol $\hat{\boldsymbol{\tau}}/c = [\mathbf{0}, \hat{\mathbf{S}}/c\,; \hat{\mathbf{S}}/c, \mathbf{0}]$ denotes the kinetic momentum operator, $c\hat{\boldsymbol{\tau}}$ is the energy flow operator, c represents the velocity of light in vacuum, $\hat{\mathbf{S}}$ indicates the spin-1 matrix in SO(3) [10, 100]. Here, the symbol * is the complex conjugate and the Dirac notation <> indicates the inner product of operator by photon wave function [100]. From the optical Dirac equation in the Riemann–Silberstein representation, the first-order time partial derivative of the position operator is $\dot{\mathbf{r}} = i[\hat{\mathbf{H}}, \mathbf{r}]/\hbar = c\hat{\boldsymbol{\tau}}$ [101–103] with $\hbar$ the reduced Plank constant, which implies that the Poynting vector/kinetic momentum reflects the (subluminal) transportation of photons in classical electrodynamics [21, 50, 78]. Alternatively, by adopting the representation as in the quantum mechanics, a so-called canonical (or orbital) momentum density can be defined from the canonical Noether theorem applied to EM fields [114–119]. This canonical momentum density is written

$$\mathbf{p_o} = \frac{1}{4\omega}\mathrm{Im}\{\epsilon\mathbf{E}^* \cdot (\nabla)\mathbf{E} + \mu\mathbf{H}^* \cdot (\nabla)\mathbf{H}\} = \frac{1}{\hbar\omega}\langle\psi|\hat{\mathbf{p}}|\psi\rangle = \frac{1}{\hbar\omega}\langle\hat{\mathbf{p}}\rangle, \tag{3}$$

where $\mathbf{X}\cdot(\nabla)\mathbf{Y} \equiv \Sigma_i x_i \nabla y_i$ and $\hat{\mathbf{p}} = -i\hbar\nabla$ denotes the momentum operator in quantum mechanics. Compared with the kinetic momentum density given by the Poynting vector, the canonical momentum density has an intuitively clear physical interpretation, specifically, it is proportional to the local gradient of the phase of the EM field, i.e., the mean wavevector $\langle\mathbf{k}\rangle = \mathbf{p_o}/\hbar$ [100, 119–122]. The canonical momentum density is independent of the polarization in uniformly polarized fields and is equally defined for a scalar wave field [123]. It coincides with the kinetic momentum only in situations in which one can neglect the polarization ellipticity or SAM. The circulation of the canonical momentum immediately yields the orbital angular momentum (OAM) density of the EM field, expressly, $\mathbf{L} = \mathbf{r} \times \mathbf{p}_o$. This density has intrinsic and extrinsic parts associated with the optical vortex and photon trajectory, respectively [4–17].

In addition, from the SAM and OAM decomposition [10, 100], the kinetic momentum density can be decomposed into $\mathbf{p} = \mathbf{p}_o + \mathbf{p}_s$, where the "spin momentum density" $\mathbf{p}_s$, which was introduced by Belinfante in field theory [124], is related to the ellipticity of polarization; expressly,

$$\begin{aligned}\mathbf{p_s} &= \frac{1}{2}\nabla \times \mathbf{S} \text{ and } \mathbf{S} = \frac{1}{4\omega}\mathrm{Im}\{\epsilon(\mathbf{E}^* \times \mathbf{E}) + \mu(\mathbf{H}^* \times \mathbf{H})\} \\ &= \frac{1}{\hbar\omega}\langle\psi|\hat{\mathbf{S}}|\psi\rangle = \frac{1}{\hbar\omega}\langle\hat{\mathbf{S}}\rangle, \end{aligned} \tag{4}$$

where $\mathbf{S}$ is the SAM seen to be proportional to the local ellipticity of the field polarization, with the spin vector lying along the normal direction of the polarization ellipse. Thus, the SAM density $\mathbf{S}$ is an independent dynamical property of the EM field, related to the polarization ellipticity of freedom [58]. Obviously, the SAM density is an intrinsic quantity, but its direction with respect to the wave momentum (whether the kinetic momentum or the canonical momentum) is not specified in the generic case. This suggests that the photonic spin vector associated with the three-dimensional rotating of electric and magnetic polarizations can be oriented in an arbitrary direction and thus contains components both perpendicular and parallel to the mean wavevector. The total AM density of the field is the sum of the spin and orbital parts: $\mathbf{J} = \mathbf{S} + \mathbf{L}$ [115, 125]. The spin and orbital AMs both manifest in very different manners in local light–matter interactions, and hence they should be considered as independent physical properties, corresponding to different degrees of freedom.

3 Theories for describing the optical transverse spin

To illustrate the different types of optical spin and the coupling with OAM, we first consider a circularly polarized plane wave propagating along the z-direction in free space with wave vector k. By expressing the electric field of the circularly polarized wave as $\mathbf{E}^{pw} = \sqrt{\hbar\omega/\epsilon_0}(1, \sigma i, 0)e^{ikz}$ in the Cartesian coordinates with unit vectors $(\hat{\mathbf{x}}, \hat{\mathbf{y}}, \hat{\mathbf{z}})$, the main dynamical quantities are found to be

$$\begin{aligned} &\mathbf{p}^{pw} = \frac{cW}{c^2}\hat{\mathbf{z}} = \mathbf{v}_g^{pw}\frac{W}{c^2} \quad \mathbf{p}_o^{pw} = \frac{cW}{c^2}\hat{\mathbf{z}} = \mathbf{v}_{go}^{pw}\frac{W}{c^2} \quad \mathbf{p}_s^{pw} = 0 \\ &W = \hbar\omega \qquad \mathbf{k}^{pw} = \frac{\mathbf{p}_o^{pw}}{\hbar} = \frac{W}{\hbar\omega}k\hat{\mathbf{z}} \quad \mathbf{S}^{pw} = \hbar\sigma\hat{\mathbf{k}}^{pw} \end{aligned}, \tag{5}$$

where ε_0 is the permittivity in vacuo and $\hat{\mathbf{k}}^{pw} = \mathbf{k}^{pw}/k$ is the unit directional vector of canonical momentum, indicating that the SAM vector is along the direction of the canonical momentum/mean wavevector, manifesting as a longitudinal-type of optical spin that is related to the EM helicity σ [126–134]. Note that both the kinetic and canonical momenta determine the velocities associated with energy transports, i.e., kinetic and canonical group velocities [50, 78, 135, 136]. For the circularly polarized light in free space, the kinetic group velocity $\mathbf{v}_g^{pw}$ and the canonical group velocity $\mathbf{v}_{go}^{pw}$ are equivalent and equal to the velocity of light c in vacuo. In addition, the spin momentum densities $\mathbf{p}_s$ of these plane waves vanish despite the beams carrying the l-SAM. However, for a structured light field, the kinetic group velocity $\mathbf{v}_g^{pw}$ regarded as the actual transportation velocity of photons will be different from the canonical group velocity $\mathbf{v}_{go}^{pw}$ which becomes superluminal contradiction to relativity [78] owing to the present of spin momentum density (generally, spin momentum is inverse to the canonical momentum to keep the actual energy transportation subluminal). Thus, the canonical group velocity $\mathbf{v}_{go}^{pw}$ is not the real velocity of photon transport but be mainly mathematical.

The situation is remarkably different when the plane wave is confined at an interface (evanescent wave) [77]. Considering a transverse magnetic-type evanescent plane wave (in Figure 3a) propagating along the y-axis and decaying in the z-direction with a complex wavevector $\mathbf{k}^{epw} = \beta\hat{\mathbf{y}} + ik_z\hat{\mathbf{z}}$, where β and ik_z stands for the in-plane and out-of-plane wavevector components and satisfy $\beta^2 - k_z^2 = k^2$. The electric and magnetic field components may be expressed as $\mathbf{E}^{epw} = \sqrt{2\hbar\omega/\epsilon_0}(0, -ik_z/\beta, 1)e^{i\beta y - k_z z}$ and $\mathbf{H}^{epw} = \sqrt{2\hbar\omega/\epsilon_0}(k/\beta, 0, 0)e^{i\beta y - k_z z}/\eta$, respectively, with the wave impedance $\eta = \sqrt{\mu_0/\epsilon_0}$; the other dynamical quantities can subsequently be obtained,

$$\begin{aligned} &\mathbf{p}^{epw} = \left(\frac{k}{\beta}c\right)\frac{W^{epw}}{c^2}\hat{\mathbf{y}} = \mathbf{v}_g^{epw}\frac{W^{epw}}{c^2} \quad \mathbf{p}_\mathbf{o}^{epw} = \left(\frac{\beta}{k}c\right)\frac{W^{epw}}{c^2}\hat{\mathbf{y}} = \mathbf{v}_{go}^{epw}\frac{W^{epw}}{c^2} \quad \mathbf{p}_\mathbf{s}^{epw} = \left(-\frac{k_z^2}{\beta k}c\right)\frac{W^{epw}}{c^2}\hat{\mathbf{y}} \\ &W^{epw} = \hbar\omega e^{-2k_z z} \qquad \mathbf{k}^{epw} = \frac{\mathbf{p}_\mathbf{o}^{epw}}{\hbar} = \frac{W^{epw}}{\hbar\omega}\beta\hat{\mathbf{y}} \qquad \mathbf{S}^{epw} = \frac{W^{epw}}{\hbar\omega}\hbar\left(\frac{k_z}{\beta}\right)\hat{\mathbf{x}} \end{aligned}. \tag{6}$$

Equation (6) reveals the transverse nature of the SAM in the evanescent plane wave (perpendicular to mean wavevector $\mathbf{k}^{epw}$). This t-SAM existed even in the single polarized light free from polarization coupling and is independent of the EM helicity σ represents a novel type of optical SAM that is in sharp contrast with the usual longitudinal-type SAM of circularly polarized plane wave. Later, the optical transverse spin indeed was also found to prevail in confined or structured EM fields in free space along with the evanescent waves, including focused beams [21, 22, 54, 55, 58], interference fields [59], and guided modes [50–52, 57, 60], and even nonpolarized light [61], to name but a few (Figure 3). The introduction of various types of optical transverse spins can be found in several other literature reviews [21, 22]. Note that the spin part of the momentum densities $\mathbf{p}_s$ of the structured lights mentioned above appear indeed, which contrasts with the case of longitudinal-type spin in circularly polarized light proportional to EM helicity σ as indicated in Eq. (5). Thus, the appearance of spin momentum density always accompanies the structured property of EM field and leads to the present of the optical transverse spin. In turn, it would play an important role in identifying and determining the optical transverse spin. (Mathematically, if the SAM $\mathbf{S}$ is purely longitudinal and parallel to the kinetic momentum $\mathbf{p}$, the spin momentum $\mathbf{p}_s = \nabla \times \mathbf{S}/2$ should be perpendicular to the $\mathbf{p}$ owing to the curl operator. This is illogical since $\mathbf{p} = \mathbf{p}_o + \mathbf{p}_s$, where the spin momentum cannot purely perpendicular to kinetic momentum [58, 95]. On the other hand, if the SAM $\mathbf{S}$ is perpendicular to the kinetic momentum $\mathbf{p}$, one can observe that the spin momentum $\mathbf{p}_s = \nabla \times \mathbf{S}/2$ is parallel to the $\mathbf{p}$.)

Previously, an empirical procedure to identify the optical transverse spins included calculating the SAM and comparing the spin orientation to the mean wavevector (or to the canonical momentum $\mathbf{p}_o$) [21, 67]. This empirical perspective, although providing an intuitive way to identify the transverse spin in various optical configurations as those demonstrated in Figure 3, cannot provide a quantitative analysis of the t-SAM, and be generalized to more complex scenarios. An example is when structured waves with an arbitrary trajectory (such as surface Airy beams, surface Weber beams, etc.) and spin–orbit coupling (such as surface Bessel beams) need to be considered for which

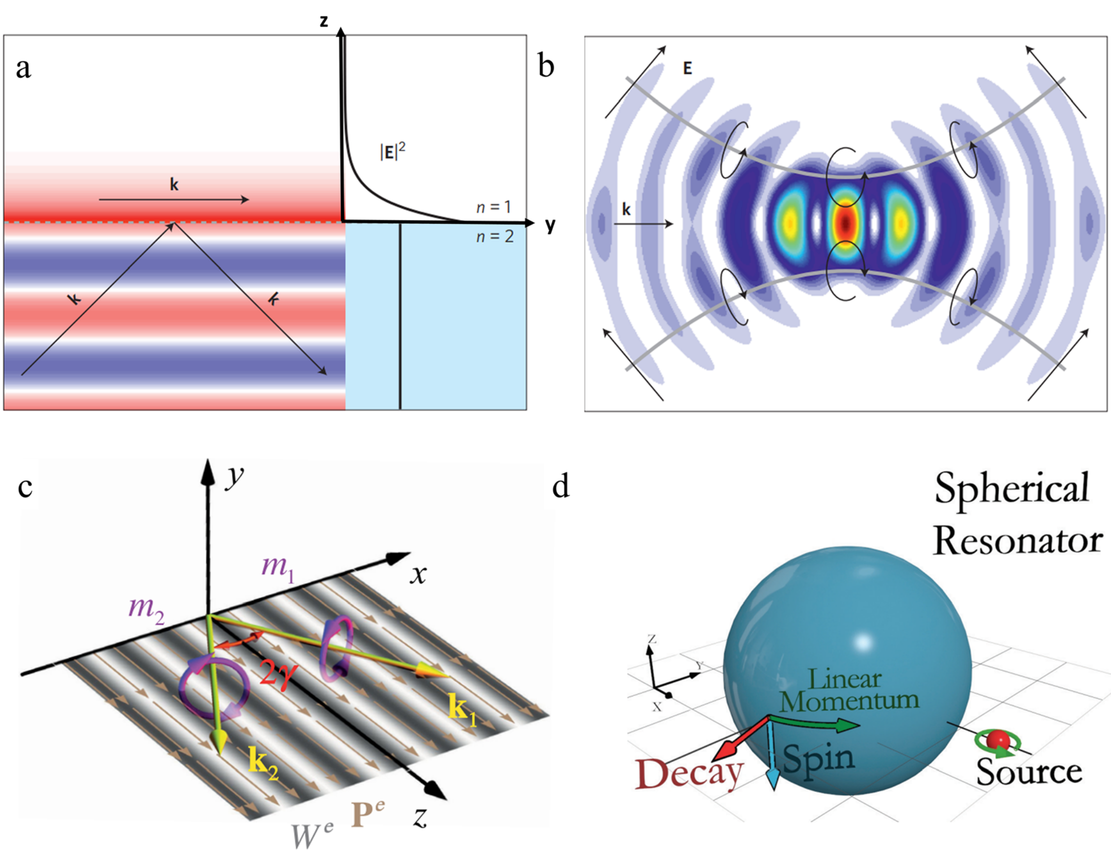

Figure 3: Identifying the transverse spin using the "$\boldsymbol{k}$-method" in various optical configurations: (a) single polarized evanescent wave [50]; (b) focused single polarized Gaussian beam [22]; (c) two-waves interference field [58, 59], and (d) whispering-gallery-mode in optical resonators [56].

the spin momentum density ($\mathbf{p}_s$) is also important [57, 78]. Based on the former analysis, the latest researches suggested that the kinetic momentum $\mathbf{p} = \mathbf{p}_o + \mathbf{p}_s$ proportional to the energy flow/Poynting vector $\mathbf{P}$ was employed for identifying and evaluating the optical transverse spins at the more general circumstances, from the purely transverse magnetic/electric surface modes [57] to an arbitrary polarized field no matter whether in the optical near-field or the free space [58].

To understand the relationship between transverse spin and energy flow/Poynting vector, we construct a classical phenomenological model analogous to fluid dynamics [137], in which a spherical Rayleigh particle with fixed translational movement but free rotational motion is embedded in an environment with a spavtially invariant flow density, to understand the generation of transverse torque in the system (Figure 4). We first assume an energy flow propagating along the +x-direction with the magnitude gradually increasing in the y-direction (Figure 4a). Obviously, a gradient force arising from the energy flow ($\propto \partial P_x/\partial y$) causes the immersed particle to experience a torque acting along the −z-direction and to rotate clockwise. In the same way, an energy flow along the +y-direction varying in the x-direction (see Figure 4b) produces a torque along the +z-direction ($\propto \partial P_y/\partial x$) and forces the particle to rotate anticlockwise. Combining these two effects, the strength of the particle's torque in the x–y plane is possibly determined by $(\partial P_y/\partial x - \partial P_x/\partial y)\hat{\mathbf{z}}$. Follow these ideas to consider the transverse torques caused by the gradient optical energy flows in the three-dimensional directions, the overall transverse spinning effect on the immersed particle as: $(\partial P_z/\partial y - \partial P_y/\partial z)\hat{\mathbf{x}} + (\partial P_x/\partial z - \partial P_z/\partial x)\hat{\mathbf{y}} + (\partial P_y/\partial x - \partial P_x/\partial y)\hat{\mathbf{z}}$. Now, from the former analysis, one may conjecture that the inherent transverse SAM in the system arising from the gradient of the energy flow density associated with the inhomogeneities/structure properties of light fields [57].

Recently, this conjecture was first validated by Shi and for the single polarized evanescent EM waves at an optical interface that manifested as a simple *curl*-relationship between the t-SAM and the Poynting vector/kinetic momentum density [57],

$$\mathbf{S}_t = \frac{1}{2\omega^2}\nabla \times \mathbf{P} = \frac{1}{2k^2}\nabla \times \mathbf{p}. \quad (7)$$

One can understand the relation in three aspects. First, it is worth noting that the law for spin-momentum locking, Eq. (7), only describes the dynamics of the transverse spin as present in Figure 4.

Second, in a special case that an interface is present between media with different relative permittivity and permeability to break the dual symmetry between the electric and magnetic features [57, 67, 114, 125, 127], there would be only the single polarized evanescent EM mode survives and the intrinsic connection between the spin and energy flow/momentum densities should be considered individually for transverse magnetic and transverse electric guided modes (as discussed in Refs. [57], [67] and [77]). Obviously, there is no coupling between the two polarized modes and thus there is no net EM helicity originated from the polarization ellipticity exist in the case (for example, the spin of circularly polarized light in Eq. (5) is originated

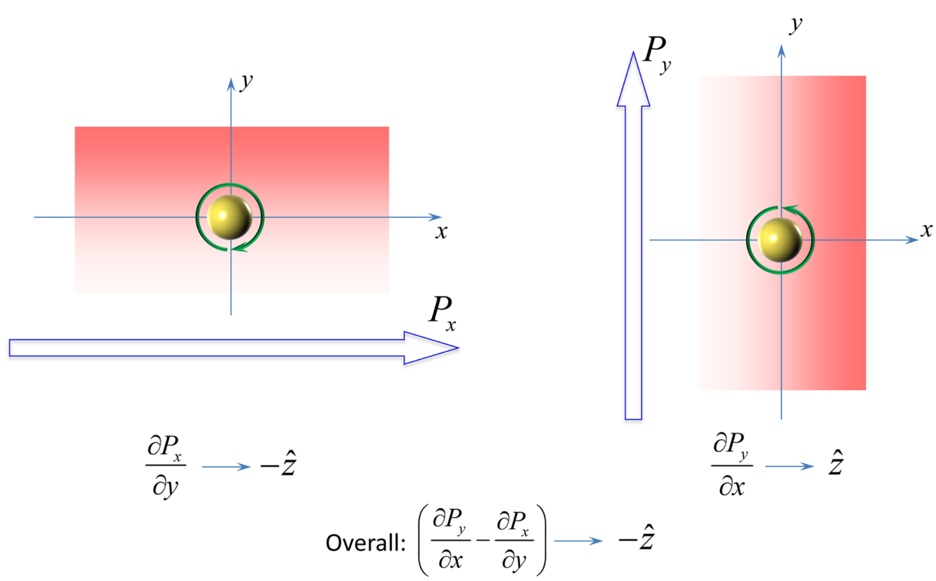

Figure 4: Classical phenomenological model analogous to fluid dynamics employed to demonstrate the relationship between transverse torque and energy flow: (a) an energy flow propagating along the +x-direction with gradually increasing magnitude in the y-direction will cause the immersed particle to rotate clockwise; (b) an energy flow propagating along the +y-direction with nonuniformity in the x-direction causes the same particle to rotate anticlockwise. The overall spinning effect on the particle is determined by factor $(\partial P_y/\partial x - \partial P_x/\partial y)\hat{\mathbf{z}}$.

from the coupling between x and y polarized modes $\mathrm{Im}\{E_x^* E_y\}$). Therefore, it is logical that the three-dimensional spin vectors of these single polarized modes can be considered as the optical transverse spin universally, namely, $\mathbf{S} = \mathbf{S}_t = \nabla \times \mathbf{P}/2\omega^2 = \nabla \times \mathbf{p}/2k^2$, which is consistent with the formula in Ref. [57]. In this way, by employing the spin–momentum relation, the optical transverse spin in the near field (Figure 3) can be evaluated analytically and quantitatively. For example, taking the evanescent plane wave propagating in the y-direction, the vorticity of the kinetic momentum is $\nabla \times \mathbf{p}^{epw} = -\partial p_y^{epw}/\partial z\hat{\mathbf{x}} = 2k^2\mathbf{S}^{epw}$, which is consistent with the former analysis in Eqs. (6) and (7). In a more general case, Eq. (7) also reveals that, in addition to the optical spin oriented along the surface (in-plane transverse SAM present in evanescent plane wave in Eq. (6)), which has been studied intensely of late, there exists another category of transverse spin for an evanescent field oriented out of the surface plane. This SAM is induced by the in-plane Poynting vector that arises from the gradient of the energy flow density within the interface, whereas the in-plane transverse spin arises from the gradient of the energy flow density normal to the interface. Taking the evanescent optical vortex (e-OV) at air/metal interface as an example [75], the kinetic momentum has only one component along the azimuthal direction because of the presence of an OAM in the beam ($p_\varphi \propto l\omega\epsilon\beta^2 J_l^2(\beta r)\exp(-2k_z z)/2r$). The variation of the momentum density in the z-direction induces an in-plane component of the SAM (S_r), whereas its variation in the radial direction induces an out-of-plane component (S_z). They are linked via the spin–momentum relation [75, 77, 78],

$$\begin{aligned}\nabla \times \mathbf{p} &= \left[-\frac{\partial p_\varphi}{\partial z}\hat{\mathbf{r}}, 0\hat{\boldsymbol{\varphi}}, \frac{1}{r}\frac{\partial}{\partial r}(rp_\varphi)\hat{\mathbf{z}}\right] \\ &= \frac{\omega\mu_0 l\beta^2}{r}\left[k_z J_l^2(\beta r)\hat{\mathbf{r}}, 0\hat{\boldsymbol{\varphi}}, \beta J_l(\beta r)J_l'(\beta r)\hat{\mathbf{z}}\right]e^{-2k_z z} \\ &= 2k^2\mathbf{S}_t = 2k^2\mathbf{S}. \end{aligned} \tag{8}$$

It is worth noting that the whole SAM components can be regarded as optical transverse spin for the single polarized evanescent wave field. The same analysis can also be extended to other structured evanescent waves such as the cosine beam, the Airy beam, the Weber beam and photonic counterpart spin topological defects [57, 76–79] in the air/metal interface. In other words, the in-plane and out-of-plane spin components together reflect the complete picture for transverse spin of structured guided waves. These results, however, cannot be explained explicitly by the previous analysis from considerations of the polarization or wavevector.

Thirdly, in the past, the optical transverse spins in confined EM fields (such as: surface plasmon polaritons (SPPs) at the air/metal interface) were considered as stemming from the emergence of the normal polarized field component with a $\pi/2$ phase shift with respect to the horizontal field and prompting the rotation of polarization within the plane containing the direction of propagation. This analysis from the perspective of the polarization did provide some clue to understanding the emergence of the optical transverse spin. Nevertheless, this can only give a qualitative analysis, and it is unclear physically why a confined EM field induces a $\pi/2$ phase difference between the normal and horizontal field components. The spin–momentum *curl*-relation tells us that if there is a structure in the momentum density, there will be a locally distributed transverse spin determined by Eq. (7). The appearance of a transverse spin indicates the rotation of polarization and hence the phase difference between the field components. Note that this theory can be used to explain the rotation of the polarization associated with all field components, rather than only between the normal and horizontal field components. More importantly, it is well-known that the longitudinal spin in the circularly polarized plane wave is determined by the EM helicity. On the contrary, the transverse spin is pervasive in the structured light field and is originated from the inhomogeneities/structure properties of classical field, including the intensity, phase, polarization and even helical inhomogeneities, as shown in Eq. (7). In addition, the other fundamental properties of t-SAMs for these single polarized modes, including the helix-free, integral vanishing and irrelative to geometric phase evolution of EM system, are totally counterintuitive and dramatically different from those of longitudinal-type spin.

Remarkably, the spin–momentum relation can also be employed for analyzing the optical transverse spin of EM fields in free space. Taking the two-wave interference of individual single polarized plane wave whose the longitudinal spin is absent (Figure 3c) as an example [21, 59], the two individual helix-free waves propagating in the xz-plane are expressed as $\mathbf{E}_1 = (k_z/k\hat{\mathbf{x}}, 0\hat{\mathbf{y}}, -k_x/k\hat{\mathbf{z}})e^{i\mathbf{k}_1\cdot\mathbf{r}}$ and $\mathbf{E}_2 = (k_z/k\hat{\mathbf{x}}, 0\hat{\mathbf{y}}, k_x/k\hat{\mathbf{z}})e^{i\mathbf{k}_2\cdot\mathbf{r}}$ with $\mathbf{k}_1 = k_z\hat{\mathbf{z}} + k_x\hat{\mathbf{x}}$ and $\mathbf{k}_1 = k_z\hat{\mathbf{z}} - k_x\hat{\mathbf{x}}$, respectively. The kinetic momentum is $\mathbf{p} = \epsilon_0 k_z\cos^2(k_x x)/2\omega\hat{\mathbf{z}}$ and the SAM is $\mathbf{S} = \epsilon_0 k_x k_z\sin(2k_x x)/4\omega k^2\hat{\mathbf{y}}$. One readily derives

$$\begin{aligned}\nabla \times \mathbf{p} &= \left[\frac{\partial p_z}{\partial y}\hat{\mathbf{x}}, -\frac{\partial p_z}{\partial x}\hat{\mathbf{y}}, 0\hat{\mathbf{z}}\right] \\ &= \left[0\hat{\mathbf{x}}, \frac{\epsilon_0 k_x k_z}{2\omega}\sin(2k_x x)\hat{\mathbf{y}}, 0\hat{\mathbf{z}}\right] = 2k^2\mathbf{S}_t = 2k^2\mathbf{S}. \end{aligned} \tag{9}$$

The same relation can also be obtained at the focal plane of a paraxial focused Gaussian beam without a longitudinal helical spin (the single polarized mode). The aforementioned examples can validate that the total spin vector of a single polarized structured light can be regarded as optical transverse spin universally that is originated from the inhomogeneity of optical field and expressed as $\mathbf{S} = \mathbf{S}_t = \nabla \times \mathbf{P}/2\omega^2 = \nabla \times \mathbf{p}/2k^2$.

Moreover, even for a generic EM field with coupled polarizations or the nonpolarized light [61], the expression (7) is also available. For example, a monochromatic circularly polarized plane-wave, Eq. (5), carries a SAM aligned parallel to the mean wavevector, whereas the curl of the Poynting vector vanishes because of the uniform distribution of the momentum density over the whole space. Thus, one can conclude that the transverse spin is zero $\mathbf{S}_t^{pw} = \nabla \times \mathbf{p}^{pw}/2k^2 = 0$ and the remaining spin can be regarded as the longitudinal-type SAM $\mathbf{S}_l^{pw} = \mathbf{S}^{pw} - \mathbf{S}_t^{pw} = \hbar\sigma\mathbf{k}^{pw}/k = \hbar\sigma\hat{\mathbf{k}}^{pw}$ in Eq. (5). Subsequently, considering an evanescent plane wave with coupling polarizations with electric field components expressed as $\mathbf{E}^{epw} = \sqrt{\hbar\omega/\epsilon_0}\left(1\hat{\mathbf{x}} - \sigma i\frac{ik_z}{k}\hat{\mathbf{y}} + \sigma i\frac{\beta}{k}\hat{\mathbf{z}}\right)e^{i\beta y - k_z z}$, the magnetic field components can be obtained as $\mathbf{H}^{epw} = \sqrt{\hbar\omega/\epsilon_0}\left(\sigma i\hat{\mathbf{x}} + \frac{ik_z}{k}\hat{\mathbf{y}} - \frac{\beta}{k}\hat{\mathbf{z}}\right)e^{i\beta y - k_z z}/\eta$. One readily derives the dynamical properties of field can be summed as: the energy density $W = \hbar\omega\frac{\beta^2}{k^2}e^{-2k_z z}$, the kinetic momentum is $\mathbf{p}^{epw} = \frac{k}{\beta}\frac{W}{c}\left(-\frac{k_z}{k}\sigma\hat{\mathbf{x}} + 1\hat{\mathbf{y}} + 0\hat{\mathbf{z}}\right)$, the transverse spin is given by $\mathbf{S}_t^{epw} = \nabla \times \mathbf{p}^{epw}/2k^2$, the longitudinal-type SAM is $\mathbf{S}_l^{epw} = \hbar\sigma\mathbf{k}^{epw}/k = \hbar\sigma\hat{\mathbf{k}}^{epw}$ and the total spin $\mathbf{S}^{ew} = \mathbf{S}_t^{ew} + \mathbf{S}_l^{ew}$ [58]. Obviously, the total spin can be decomposed into longitudinal and transverse spins, where the transversality of transverse spin is available universally because there must be $\nabla\bullet\nabla \times \mathbf{A} = 0$ for an arbitrary vector $\mathbf{A}$. Furthermore, to generalize this idea to a more general situation, we consider the two-waves interference in which the two individual interfering waves can be linear, elliptical or circular polarization. From laborious derivations, it can be obtained that the expression (7) for transverse spin still satisfies, which indicates that the total SAM of the field can be decomposed into the transverse spin generated by the structure properties of the EM field $\mathbf{S}_t = \nabla \times \mathbf{p}/2k^2$ and, together with the longitudinal spin determined by the EM helicity solely $\mathbf{S}_l = \hbar\sigma \wedge \hat{\mathbf{k}}$ [58]. Here, the symbol $\wedge$ represents the interconnection between the helicity and wavevector is local instead of global. Noteworthily, the decomposition of spin into the transverse and longitudinal spins is in accord with the Helmholtz decomposition of an arbitrary vector field. From the superposition theory of states, an arbitrarily structured light field can be expanded into the superposition of plane waves [1, 2]. Thus, our result can be also available in the arbitrarily structured light field that can be decomposed into the superposition of plane waves [58]. To sum, the expression (7) describes the dynamics of the transverse spin of the structured EM field, no matter whether in the near-field or in free space.

In addition, Eq. (7) also indicates that the transverse spin has no source, i.e., $\nabla\cdot\mathbf{S_t} = 0$. In consequence, for guided EM waves without a longitudinal-type optical spin (since we will consider the photonic chiral spin textures in this situation), a set of spin-momentum equations may be formulated analogous to the Maxwell equations (Table 1: here, for the single polarized mode without a longitudinal-type optical spin, the total SAM is consistent with the t-SAM and we ignore the subscript t in the symbol $\mathbf{S}$). Bearing in mind that an EM wave in a source-free homogeneous medium may be described using a Hertz potential (Ψ) satisfying the wave equation: $\nabla^2\Psi + k^2\Psi = 0$, and that the Poynting vector ($\mathbf{P} = c^2\mathbf{p}$) may be calculated from the Hertz potential, $\mathbf{P} \propto i(\Psi^\star\nabla\Psi - \Psi\nabla\Psi^\star)$ [123], one finds that the spin and orbital properties of the guided EM modes may be obtained directly from the spin–momentum equations without knowledge of the electric and magnetic fields. This framework opens up opportunities for designing spin structures and topological properties of EM waves with practical importance in spin optics, topological photonics, metrology and quantum technologies, and may be used to extend the spin-dynamics concepts to fluid, acoustic, and gravitational waves [138–143].

Furthermore, following the same operations performed on Maxwell's equations, one can obtain a Helmholtz-like equation that describes the spin–orbit coupling of guided EM fields (see row 7 in Table 1). From the row 5, one can find that, comparing to the electric currents (**J**) in Maxwell's equations are considered as external sources for magnetic field (**H**) (Ampere's Law), the

Table 1: Spin-momentum equations for the single polarized EM evanescent waves [54].

Spin-momentum equations
$\nabla \cdot \mathbf{p} = 0$
$\nabla \cdot \mathbf{S} = 0$
$\nabla \times \mathbf{p} = 2k^2\mathbf{S}$
$\nabla \times \mathbf{S} = 2(\mathbf{p} - \mathbf{p}_o)$
Helmholtz-like equation
$\nabla^2\mathbf{S} + 4k^2\mathbf{S} = 2\nabla \times \mathbf{p}_o$

orbit part of the momentum density ($\mathbf{p}_o$), which determines the OAM of the field ($\mathbf{L} = \mathbf{r} \times \mathbf{p}_o$) [20], is considered here as an internal competitor of optical transverse spin (On one hand, due to the conservation of total angular momentum, the Helmholtz equation represents the conversation from the OAM $\mathbf{L} = \mathbf{r} \times \mathbf{p}_o$ to the SAM expressed by $\mathbf{r} \times \mathbf{p}_o$ in Ref. [20]. On the other hand, the Helmholtz-like equation in row 7 can be also considered as the spin-momentum locking between canonical momentum and SAM). Although the total momentum $\mathbf{p} = \mathbf{p}_o + \mathbf{p}_s \propto \hbar k$ is definite for a monochromatic photon, the local structure or varying of the canonical momentum density ($\mathbf{p}_o$) will affect the redistribution of optical transverse spin and hence the accompanied spin momentum density (because the photon momentum $\hbar k$ is constant), which can be considered as a mechanism that the canonical momentum density is in competition with the spin momentum density through the interchange between the two kinds of angular momenta (spin and orbital) [78].

4 Topological properties of optical transverse spin

In addition to uncover the physical dynamics of transverse spin, Eq. (7) indicates a unique spin-momentum locking feature associated with this spin. For the evanescent plane wave at a vacuum/metal interface (Figure 5a) and from Eq. (5), oppositely propagating evanescent waves with $+\mathbf{p}$ and $-\mathbf{p}$ along the y-direction carry opposite transverse optical spins $\mathbf{S}_x > 0$ and $\mathbf{S}_x < 0$ along the x-direction, with the direction of the t-SAM locked to the kinetic momentum of the wave. This universal feature of spin–momentum locking is considered a photonic analog to the quantum spin-Hall effect of electrons in topological insulators [144–149]. This feature underlies the spin-controlled directional coupling of evanescent waves such as SPPs [19, 20, 57, 58, 62–68, 83–94]. For structured evanescent waves with spatially varying intensity distributions, inhomogeneity in

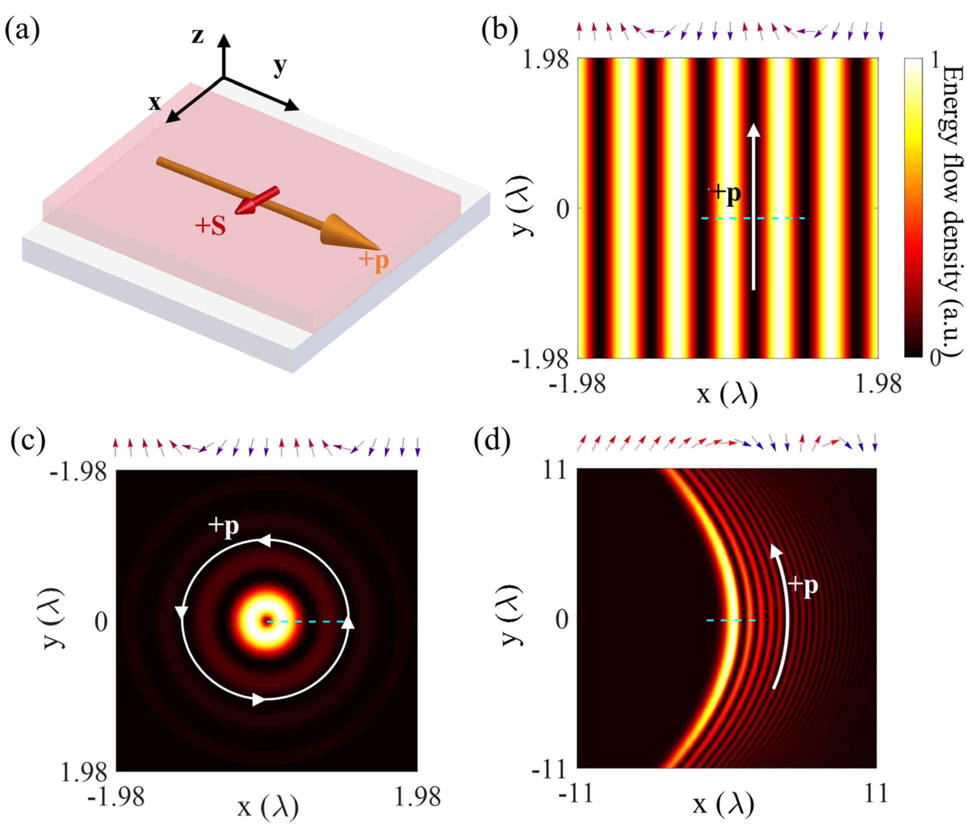

Figure 5: Transverse spins and spin–momentum locking in various evanescent SPP waves arising from the spatial variation of the kinetic momentum/Poynting vector: (a) in an unstructured evanescent plane wave, an in-plane transverse spin is present because the Poynting vector normal to the interface decays [67]; (b–d) in structured evanescent waves such as (b) the cosine wave, (c) the Bessel wave, and (d) the Airy wave, there exists besides the in-plane transverse SAM as in (a), another type of transverse spin aligned normal to the interface that is induced by the in-plane Poynting vector arising from the variation in energy flow density within the interface. The spin vectors of the structured beams swirl around the energy flow lobes and their local orientations vary from the 'up' to the 'down' states, obeying the right-hand rule (see inserts above the panels; the vector graphs show the normalized spin vector along the green lines in the corresponding figures). These orientations are inverted for waves with an opposite direction to the energy flow. Note that for beams with curved trajectories, the spin variation is considered in the plane perpendicular to the local tangential direction of the energy flow [57].

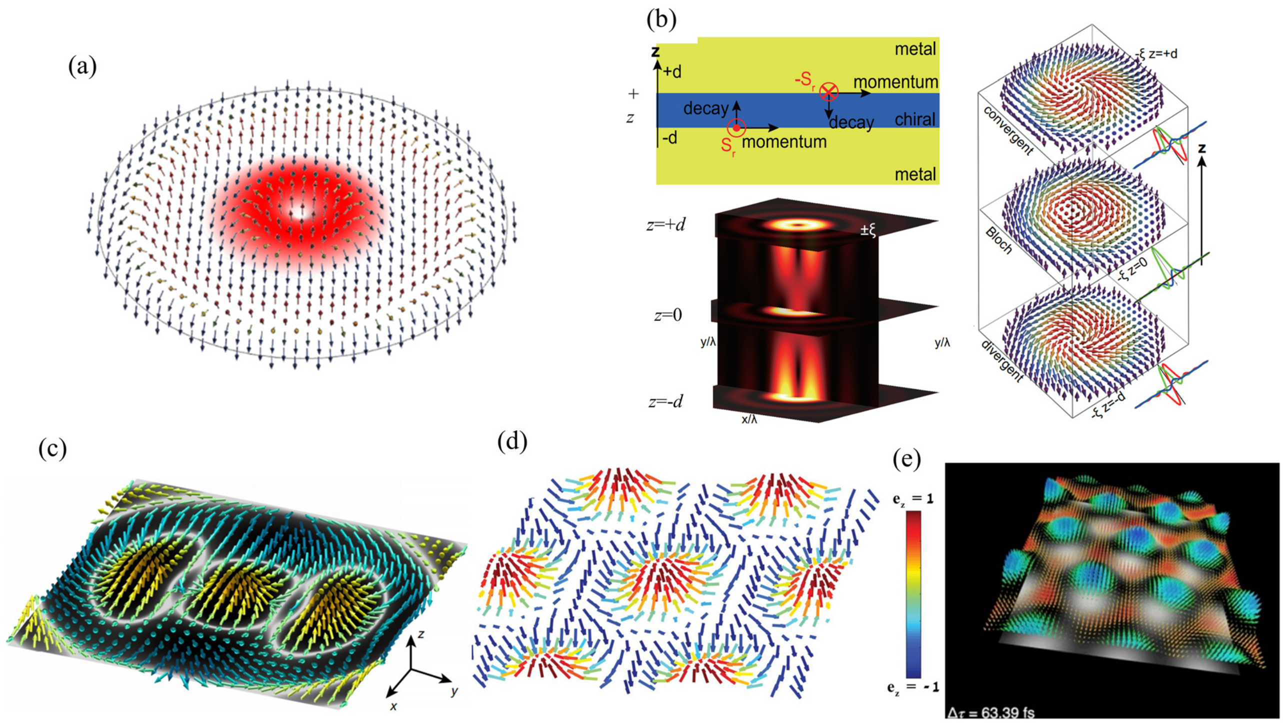

Figure 6: Various kinds of photonic topological structures in guided waves formed in real space: (a) Néel-type photonic spin skyrmion formed in an evanescent optical vortex, for which the spin vector varies progressively from the 'up/down' state at the center to the 'down/up' state at the edge (with integer skyrmion number) [75]; (b) Bloch-type photonic spin skyrmion in guided waves introduced into a layer of a chiral material which induces an **E**–**H** coupling [141]; (c) meron-like photonic spin structure in a specially designed SPP field [156]; (d) and (e) lattices exhibiting 6-fold rotational symmetry of dynamic field skyrmions produced by an evanescent field in the absence spin–orbit coupling, mapped (d) spatially [154] and (e) temporally [155].

the momentum density induces both in-plane and out-of-plane *t*-SAM components introduced above. Both are perpendicular to the local direction of momentum. The relationship between the two components leads to a chiral spin texture with spin vectors swirling around the momentum lobe (Figure 5b–d), its directional variation (i.e., chirality) being locked with the momentum. The orientation of the spin vectors varies progressively from the 'up' state to the 'down' state across the momentum lobes while obeying the right-hand rule (at the vacuum half space). This progression is a manifestation of a generalized spin–momentum locking associated with an arbitrary structured evanescent wave.

Definitely, the total Chern number of a surface mode vanishes ($C_t = 0$) originated from the time-reversal symmetry of nonmagnetic Maxwell's equations [57, 67, 77]. However, the spin Chern number is $C_{spin} = 4$. This nonzero spin Chern number implies that the nontrivial helical states of EM waves indeed exist and are strictly locked to the energy propagation direction [57]. Despite the existence of such nontrivial helical states at the interface governed by the spin-momentum locking, the topological $\mathbb{Z}_2$ invariant of these states vanishes owing to the time-symmetry of the Maxwell's equations. Thus, the spin-momentum locking of optical transverse spin discussed here is different from the "pseudo-spin" [147–149] in artificial photonic structures which is engineered to break the time-reversal symmetry, therefore, possessing protection against back-scattering. Although the transformation of the two helical states of evanescent waves is not topologically protected against scattering, the spin-momentum locking and the induced unidirectional excitation and transportation of photons are the intrinsic feature of the Maxwell's theory and are topological nontrivial (possess $\mathbb{Z}_4$ topological invariant) [57, 77, 150].

Note that the spin vector has an orientation along the interface at the maxima of the momentum density and are normal to the interface at the nodes. Therefore, a period for the spin variation can be defined with respect to two adjacent nodes of the kinetic momentum density as exhibited by topological solitons [75–81, 151–159]. This results in the formation of many intriguing photonic spin structures arising from spin–orbit coupling, for example, the Néel-type photonic spin skyrmion in an evanescent optical vortex [75–81] (Figure 6a), the Bloch-type skyrmion in the presence of a layer of chiral material [151] (Figure 6b), and the meron-like spin structure in a specially designed structured field [156] (Figure 6c). In the absence of spin–orbit coupling though, these spin topologies degenerate into dynamic field-skyrmions [154, 155] (Figure 6d and e). These intriguing topological structures in real space and their ultrafast dynamics have attracted wide interest recently and open up new pathways for topological photonics, quantum photonics and metrology, and new avenues to explore topological condensed matter systems [160–162].

5 Experimental characterization of transverse spin

In contrast to the longitudinal spin of circularly polarized light in free space, the measurement of the transverse spin density of evanescent waves or strongly confined EM fields requires more elaborate detection techniques having nanoscale precision [54, 55, 57, 58, 61, 66, 76, 81, 82, 152–156, 163–167]. To characterize the transverse SAM in confined EM fields, much effort has been spent in the past few years yielding several techniques. Banzer and colleagues proposed and demonstrated a self-built optical detection system that employs a SiO_2-coated silicon nanoparticle as a near-field probe (Figure 7a) [55]. High refractive index nanoparticles such as Si-nanoparticles support both electric and magnetic resonances. When interacting with an incident beam, scattering emissions from the nanoparticles exhibit a certain directionality related to the transverse spin. By extracting the intensity information at four specific points in $\boldsymbol{k}$-space (back focal plane), the transverse SAM density may be reconstructed by employing the dipole theorem, both for the electric and magnetic parts of the transverse SAM density. Employing this method, the transverse spin in focused cylindrical vector beams associated with the longitudinal field component (E_z or H_z), i.e., the in-plane t-SAM, was measured successfully (Figure 7b).

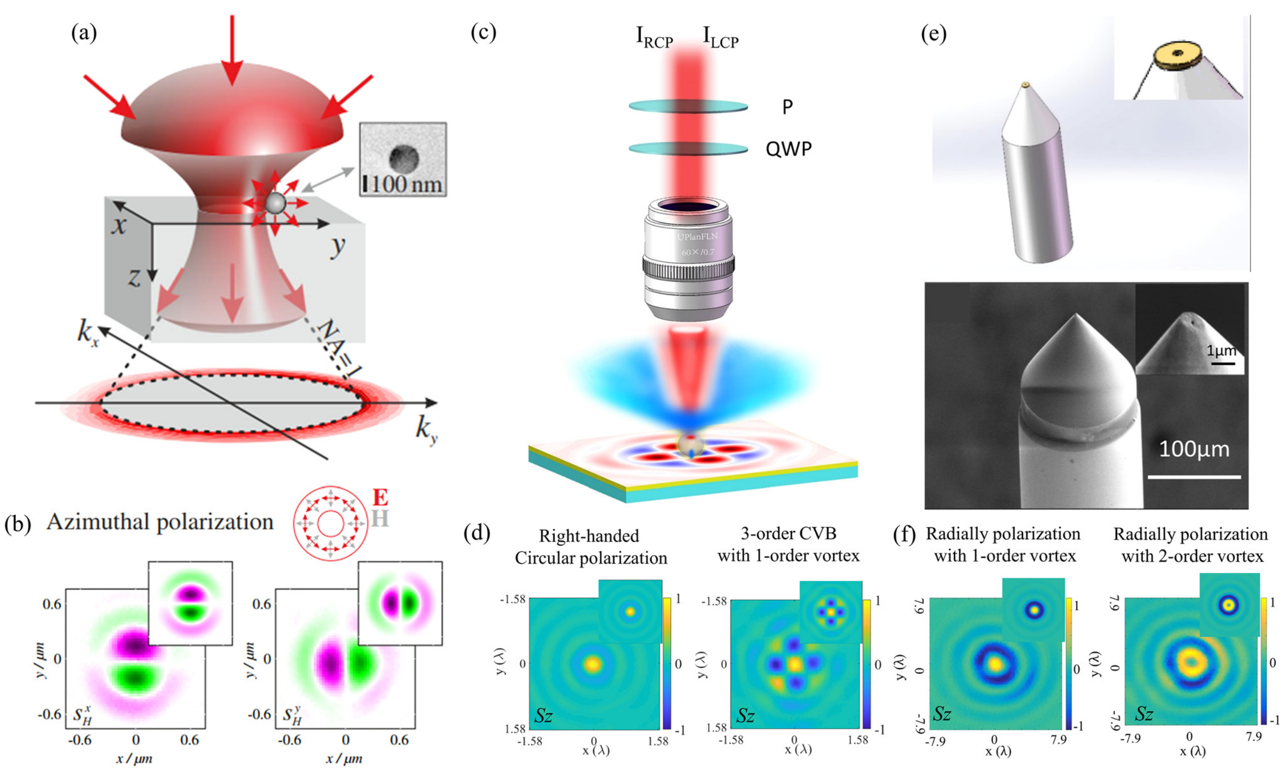

Figure 7: Experimental tools developed for measuring the transverse SAM: (a) and (b) a Si-nanoparticle, of which the scattering pattern at the Fourier domain is related strongly to the transverse spin, was employed for measuring the transverse SAM density of focused vector beams associated with the longitudinal fields (i.e., the in-plane transverse spin) [55]. (c) and (d) A nanoparticle-on-film structure, designed to be sensitive to the transversal field component, was employed to map the near-field distribution of the out-of-plane transverse SAM component of SPPs [76]. (e) and (f) A tapered fiber probe sensitive to the transversal field was employed to map the out-of-plane SAM component of various focused cylindrical vector beams [166].

Besides the in-plane *t*-SAM component, several researchers proposed a configuration to map the out-of-plane *t*-SAM component in SPPs (Figure 7c) [57, 76]. The method is based on an inherent relationship between the out-of-plane SAM and the two circular polarization components of the in-plane field: $S_z \propto I_{RCP} - I_{LCP}$. In their experiments, a nanoparticle-on-film structure was employed as a near-field probe, to be sensitive specifically to the in-plane electric field component. A combination of a quarter waveplate and a polarizer was used to extract the two circular polarization components of the far-field signal. The configuration was employed to map the near-field distributions of the out-of-plane SAM component for various structured SPP fields (Figure 7d). This method is consistent with the techniques in reference [64].

The above method was later extended and adopted in a scanning near-field optical microscope (Figure 7e) to map the out-of-plane SAM component in various focused cylindrical vector beams [166]. A tapered fiber probe coated with 200 nm-thick gold film with a nano-hole punched at the end face is sensitive specifically to the transversal field. Using a quarter-wave plate and a linear polarizer to analyze the collected signals as above, the CP components associated with the transversal field component may be extracted to reconstruct the longitudinal SAM component, in principle for any arbitrary EM field (Figure 7f).

6 Conclusions and prospects

We reviewed the recent progress in spin photonics associated with transverse spins, with an emphasis on introducing their underlying physical dynamics, their topological properties, and resultant structures. The optical transverse spins originate within the spatial structure of the kinetic momentum/energy flow and are a fundamental property of EM waves. In contrast to the longitudinal-type spin in circularly polarized light, which typically requires a "source" for their generation (e.g., birefringent or chiral materials), the transverse spin is source-less and hence exists widely in structured or confined EM fields with nonuniform intensity distributions. The curl-relationship with the kinetic momentum density results in a set of Maxwell-like spin–momentum equations that link the spin and OAM in guided near-field waves. With these equations, the spin and orbit AMs are obtained directly from the scalar Hertz potential of an optical system, without knowing the electric and magnetic fields. As a result, although being a parameter related to polarization, the modulation of the transverse spin in guided waves may be performed independently of the polarization. Indeed, the control and modulation of the SAM in the past from the perspective of polarization is difficult as polarization is a vectorial parameter, particularly in strongly confined EM fields where the intensity, phase, and polarization are strongly related. With this consideration, the transverse spin may be a degree of freedom having both wide modulation and broad application. For example, based on the deep-subwavelength feature of fine structure in photonic skyrmion, one can develop a metrology technique with sub-nm resolution, which has potential for applications in the single molecule localization imaging [75]. On the other hand, based on the chiral whirling feature of photonic skyrmion and meron, one can predict a momentum-locked unidirectional optical force in the interaction between chiral textures and chiral molecule [78], which can be widely used in the chiral detection, chiral imaging, etc. Moreover, the photonic solitons, which are stable and protected by the symmetry of optical system, would be applied in the optical data coding and storage. In addition, the demonstration of chiral textures was relied on the various high-precision ultrafast optical near-field measurement systems. In contrast, the fast development of chiral textures would also accelerate the development of near-field measurement techniques and the further ultrafast control of photon–electron interactions [155, 156]. Through its subwavelength feature and its natural chiral property, the transverse spin may find advanced applications in optical nanometrology, chiral molecule detection and imaging, data coding and storage, and the ultrafast control of photon–electron interactions. The concept and framework regarding spin–orbit interactions and spin–orbit decomposition has been extended into a variety of classical waves, including acoustic waves [138–140], elastic [141], fluid waves [142], and even gravitational waves [143]. For example, longitudinal acoustic waves have a Klein–Gordon representation and there is a similar curl relationship between the momentum and the SAM [138–140]. This would provide new insights for interdisciplinary research covering analogies of other systems to optical systems.

Acknowledgments: Guangdong Major Project of Basic Research No. 2020B0301030009, National Natural Science Foundation of China grants U1701661, 61935013, 62075139, 61427819, 61622504, 12174266, 12047540, and 61705135, leadership of Guangdong province program grant 00201505, Natural Science Foundation of Guangdong Province grant 2016A030312010, Science and Technology Innovation Commission of Shenzhen grants RCJC20200714114435063, JCYJ20200109114018750, JCYJ20180507182035270, Shenzhen Peacock Plan

KQTD20170330110444030. L. D. acknowledges the support given by the Guangdong Special Support Program.

Author contribution: All the authors have accepted responsibility for the entire content of this submitted manuscript and approved submission.

Research funding: None declared.

Conflict of interest statement: The authors declare no conflicts of interest.

References

[1] J. D. Jackson, *Classical Electrodynamics*, 3rd ed. New Jersey, Wiley, 1999.
[2] M. Born and E. Wolf, *Principles of Optics*, 7th ed. London, Pergamon, 2005.
[3] J. H. Poynting, "The wave-motion of a revolving shaft, and a suggestion as to the angular momentum in a beam of circularly-polarized light," *Proc. R. Soc. London, Ser. A*, vol. 82, pp. 560–567, 1909.
[4] L. Allen, M. W. Beijersbergen, R. J. Spreeuw, and J. P. Woerdman, "Orbital angular momentum of light and the transformation of Laguerre-Gaussian laser modes," *Phys. Rev. A*, vol. 45, no. 11, pp. 8185–8189, 1992.
[5] L. Allen, M. J. Padgett, and M. Babiker, "The orbital angular momentum of light," *Prog. Opt.*, vol. 39, pp. 291–372, 1999.
[6] A. M. Yao and M. J. Padgett, "Optical angular momentum: origins, behavior, and applications," *Adv. Opt. Photon*, vol. 3, pp. 161–204, 2011.
[7] Y. Shen, X. Wang, Z. Xie, et al., "Optical vortices 30 years on: OAM manipulation from topological charge to multiple singularities," *Light: Sci. Appl.*, vol. 8, pp. 90:1–29, 2019.
[8] S. Franke-Arnold, L. Allen, and M. J. Padgett, "Advances in optical angular momentum," *Laser Photon. Rev.*, vol. 2, pp. 299–313, 2008.
[9] D. Mao, Y. Zheng, C. Zeng, et al., "Generation of polarization and phase singular beams in fibers and fiber lasers," *Adv. Photon.*, vol. 3, pp. 014002:1–18, 2021.
[10] A. Bekshaev, K. Y. Bliokh, and M. Soskin, "Internal flows and energy circulation in light beams," *J. Opt.*, vol. 13, pp. 053001: 1–32, 2011.
[11] J. Leach, M. J. Padgett, S. M. Barnett, S. Franke-Arnold, and J. Courtial, "Measuring the orbital angular momentum of a single photon," *Phys. Rev. Lett*, vol. 88, no. 25, pp. 257901, 2002.
[12] S. J. van Enk and G. Nienhuis, "Spin and orbital angular-momentum of photons," *Europhys. Lett.*, vol. 25, pp. 497–501, 1994.
[13] S. J. van Enk and G. Nienhuis, "Commutation rules and eigenvalues of spin and orbital angular momentum of radiation fields," *J. Mod. Opt.*, vol. 41, pp. 963–977, 1994.
[14] X. Fang, H. Yang, W. Yao, et al., "High-dimensional orbital angular momentum multiplexing nonlinear holography," *Adv. Photon.*, vol. 3, pp. 015001:1–7, 2021.
[15] C.-F. Li, "Spin and orbital angular momentum of a class of nonparaxial light beams having a globally defined polarization," *Phys. Rev. A*, vol. 80, no. 6, pp. 063814:1–11, 2009.
[16] K. Y. Bliokh, A. Niv, V. Kleiner, and E. Hasman, "Geometrodynamics of spinning light," *Nat. Photonics*, vol. 2, pp. 748–753, 2008.
[17] K. Y. Bliokh, "Geometrodynamics of polarized light: Berry phase and spin Hall effect in a gradient-index medium," *J. Opt. Pure Appl. Opt.*, vol. 11, pp. 094009:1–14, 2009.
[18] A. R. Beth, "Mechanical detection and measurement of the angular momentum of light," *Phys. Rev.*, vol. 50, pp. 115–125, 1936.
[19] K. Y. Bliokh, F. J. Rodríguez-Fortuño, F. Nori, and A. V. Zayats, "Spin–orbit interactions of light," *Nat. Photonics*, vol. 9, no. 12, pp. 796–808, 2015.
[20] P. Shi, A. Yang, F. Meng, et al., "Optical near-field measurement for spin-orbit interaction of light," *Prog. Quant. Electron.*, vol. 78, pp. 100341:1–20, 2021.
[21] K. Y. Bliokh and F. Nori, "Transverse and longitudinal angular momenta of light," *Phys. Rep.*, vol. 592, pp. 1–38, 2015.
[22] A. Aiello, P. Banzer, M. Neugebauer, and G. Leuchs, "From transverse angular momentum to photonic wheels," *Nat. Photonics*, vol. 9, no. 12, pp. 789–795, 2015.
[23] A. T. O'Neil, I. MacVicar, L. Allen, and M. J. Padgett, "Intrinsic and extrinsic nature of the orbital angular momentum of a light beam," *Phys. Rev. Lett.*, vol. 88, pp. 053601:1–4, 2002.
[24] F. Cardano and L. Marrucci, "Spin–orbit photonics," *Nat. Photonics*, vol. 9, no. 12, pp. 776–778, 2015.
[25] V. G. Fedoseyev, "Conservation laws and transverse motion of energy on reflection and transmission of electromagnetic waves," *J. Phys. A: Math. Gen.*, vol. 21, pp. 2045–2059, 1988.
[26] M. Onoda, S. Murakami, and N. Nagaosa, "Hall effect of light," *Phys. Rev. Lett.*, vol. 93, pp. 083901:1–4, 2004.
[27] K. Y. Bliokh and Y. P. Bliokh, "Conservation of angular momentum, transverse shift, and spin Hall effect in reflection and refraction of an electromagnetic wave packet," *Phys. Rev. Lett.*, vol. 96, pp. 073903:1–4, 2006.
[28] K. Y. Bliokh and F. Nori, "Relativistic Hall effect," *Phys. Rev. Lett.*, vol. 108, pp. 120403:1–5, 2012.
[29] O. Hosten and P. Kwiat, "Observation of the spin Hall effect of light via weak measurements," *Science*, vol. 319, pp. 787–790, 2008.
[30] X. Yin, Z. Ye, J. Rho, Y. Wang, and X. Zhang, "Photonic spin Hall effect at metasurfaces," *Science*, vol. 339, pp. 1405–1407, 2013.
[31] X. Ling, X. Zhou, K. Huang, et al., "Recent advances in the spin Hall effect of light," *Rep. Prog. Phys.*, vol. 80, pp. 066401:1–17, 2017.
[32] Y. Gorodetski, K. Y. Bliokh, B. Stein, et al., "Weak measurements of light chirality with a plasmonics slit," *Phys. Rev. Lett.*, vol. 109, pp. 013901:1–5, 2012.
[33] P. Deng, W. Hong, L. Gao, and H. Xu, "Strong spin-orbit interaction of light in plasmonic nanostructures and nanocircuits," *Phys. Rev. Lett.*, vol. 117, pp. 166803:1–5, 2016.
[34] H. Wang and X. Zhang, "Unusual spin Hall effect of a light beam in chiral metamaterials," *Phys. Rev. A*, vol. 83, pp. 053820:1–9, 2011.
[35] A. Aiello and J. P. Woerdman, "Role of beam propagation in Goos–Hänchen and Imbert–Fedorov shifts," *Opt. Lett.*, vol. 33, pp. 1437–1439, 2008.
[36] K. Y. Bliokh, I. V. Shadrivov, and Y. S. Kivshar, "Goos–Hanchen and Imbert–Fedorov shifts of polarized vortex beams," *Opt. Lett.*, vol. 34, pp. 389–391, 2009.

[37] M. Merano, N. Hermosa, J. P. Woerdman, and A. Aiello, "How orbital angular momentum affects beam shifts in optical reflection," *Phys. Rev. A*, vol. 82, pp. 023817:1–5, 2010.

[38] K. Y. Bliokh and A. Aiello, "Goos–Hanchen and Imbert–Fedorov beam shifts: an overview," *J. Opt.*, vol. 15, pp. 014001:1–16, 2013.

[39] H. Luo, S. Wen, W. Shu, and D. Fan, "Role of transverse momentum currents in the optical Magnus effect in free space," *Phys. Rev. A*, vol. 81, pp. 053826:1–10, 2010.

[40] K. Y. Bliokh, Y. Gorodetski, V. Kleiner, and E. Hasman, "Coriolis effect in optics: unified geometric phase and spin-Hall effect," *Phys. Rev. Lett.*, vol. 101, no. 3, pp. 030404:1–4, 2008.

[41] Y. Gorodetski, A. Niv, V. Kleiner, and E. Hasman, "Observation of the spin-based plasmonic effect in nanoscale structures," *Phys. Rev. Lett.*, vol. 101, no. 4, pp. 043903:1–4, 2008.

[42] Y. Gorodetski, S. Nechayev, V. Kleiner, and E. Hasman, "Plasmonic Aharonov-Bohm effect: optical spin as the magnetic flux parameter," *Phys. Rev. B*, vol. 82, no. 12, pp. 125433:1–4, 2010.

[43] C. N. Alexeyev and M. A. Yavorsky, "Topological phase evolving from the orbital angular momentum of 'coiled' quantum vortices," *J. Opt. A*, vol. 8, pp. 752–758, 2006.

[44] K. Y. Bliokh, "Geometrical optics of beams with vortices: Berry phase and orbital angular momentum Hall effect," *Phys. Rev. Lett.*, vol. 97, pp. 043901:1–4, 2006.

[45] S. Mei, K. Huang, H. Liu, et al., "On-chip discrimination of orbital angular momentum of light with plasmonic nanoslits," *Nanoscale*, vol. 8, pp. 2227–2233, 2016.

[46] L. T. Vuong, A. J. L. Adam, J. M. Brok, P. C. M. Planken, and H. P. Urbach, "Electromagnetic spin-orbit interactions via scattering of subwavelength apertures," *Phys. Rev. Lett.*, vol. 104, no. 8, p. 083903, 2010.

[47] Y. Zhao, J. S. Edgar, G. D. M. Jeffries, D. McGloin, and D. T. Chiu, "Spin-to-orbital angular momentum conversion in a strongly focused optical beam," *Phys. Rev. Lett.*, vol. 99, pp. 073901:1–4, 2007.

[48] K. Y. Bliokh, E. A. Ostrovskaya, M. A. Alonso, O. G. Rodríguez-Herrera, D. Lara, and C. Dainty, "Spin-to-orbital angular momentum conversion in focusing, scattering, and imaging systems," *Opt. Express*, vol. 19, no. 27, pp. 26132–26149, 2011.

[49] L. Marrucci, C. Manzo, and D. Paparo, "Optical spin-to-orbital angular momentum conversion in inhomogeneous anisotropic media," *Phys. Rev. Lett.*, vol. 96, no. 16, pp. 163905:1–4, 2006.

[50] K. Y. Bliokh and F. Nori, "Transverse spin of a surface polariton," *Phys. Rev. A*, vol. 85, no. 6, pp. 061801:1–5, 2012.

[51] P. Banzer, M. Neugebauer, A. Aiello, et al., "The photonic wheel-demonstration of a state of light with purely transverse angular momentum," *J. Eur. Opt. Soc, Rapid publ.*, vol. 8, pp. 13032:1–6, 2013.

[52] K.-Y. Kim and A. X. Wang, "Spin angular momentum of surface modes from the perspective of optical power flow," *Opt. Lett.*, vol. 40, pp. 2929–2932, 2015.

[53] K. Y. Bliokh, A. Y. Bekshaev, and F. Nori, "Extraordinary momentum and spin in evanescent waves," *Nat. Commun.*, vol. 5, no. 1, pp. 33001:1–8, 2014.

[54] M. Neugebauer, T. Bauer, A. Aiello, and P. Banzer, "Measuring the transverse spin density of light," *Phys. Rev. Lett.*, vol. 114, pp. 063901:1–5, 2015.

[55] M. Neugebauer, J. S. Eismann, T. Bauer, and P. Banzer, "Magnetic and electric transverse spin density of spatially confined light," *Phys. Rev. X*, vol. 8, pp. 021042:1–8, 2018.

[56] F. Khosravi, C. L. Cortes, and Z. Jacob, "Spin photonics in 3D whispering gallery mode resonators," *Opt. Express*, vol. 27, no. 11, pp. 15846–15855, 2019.

[57] P. Shi, L.-P. Du, C.-C. Li, A. Zayats, and X.-C. Yuan, "Transverse spin dynamics in structured electromagnetic guided waves," *Proc. Natl. Acad. Sci. U.S.A.*, vol. 118, no. 6, pp. e2018816118:1–6, 2021.

[58] P. Shi, A. Yang, X. Yin, L. Du, X. Lei, and X. Yuan, *Extraordinary Spin in a Generic Electromagnetic Field*, 2021, arXiv: 2108.00725.

[59] A. Y. Bekshaev, K. Y. Bliokh, and F. Nori, "Transverse spin and momentum in two-wave interference," *Phys. Rev. X*, vol. 5, pp. 011039:1–9, 2015.

[60] L. Peng, L. Duan, K. Wang, et al., "Transverse photon spin of bulk electromagnetic waves in bianisotropic media," *Nat. Photonics*, vol. 13, pp. 878–882, 2019.

[61] J. S. Eismann, L. H. Nicholls, D. J. Roth, et al., "Transverse spinning of unpolarized light," *Nat. Photonics*, vol. 15, pp. 156–161, 2020.

[62] D. O'Connor, P. Ginzburg, F. J. Rodríguez-Fortuño, G. A. Wurtz, and A. V. Zayats, "Spin-orbit coupling in surface plasmon scattering by nanostructures," *Nat. Commun.*, vol. 5, no. 1, pp. 53271:1–7, 2014.

[63] F. J. Rodríguez-Fortuño, G. Marino, P. Ginzburg, et al., "Near-field interference for the unidirectional excitation of electromagnetic guided modes," *Science*, vol. 340, pp. 328–330, 2013.

[64] F. J. Rodríguez-Fortuño, I. Barber-Sanz, D. Puerto, A. Griol, and A. Martinez, "Resolving light handedness with an on-chip silicon microdisk," *ACS Photonics*, vol. 1, no. 9, pp. 762–767, 2014.

[65] Z. Guo, Y. Long, H. Jiang, J. Ren, and H. Chen, "Anomalous unidirectional excitation of high-k hyperbolic modes using all-electric metasources," *Adv. Photon.*, vol. 3, pp. 036001:1–10, 2021.

[66] A.-P. Yang, L.-P. Du, F.-F. Meng, and X.-C. Yuan, "Optical transverse spin coupling through a plasmonic nanoparticle for particle-identification and field-mapping," *Nanoscale*, vol. 10, pp. 9286–9291, 2018.

[67] K. Y. Bliokh, D. Smirnova, and F. Nori, "Quantum spin Hall effect of light," *Science*, vol. 348, pp. 1448–1451, 2015.

[68] T. V. Mechelen and Z. Jacob, "Universal spin-momentum locking of evanescent waves," *Optica*, vol. 3, no. 2, pp. 118–126, 2016.

[69] C. Triolo, A. Cacciola, S. Patane, R. Saija, S. Savasta, and F. Nori, "Spin-momentum locking in the near field of metal nanoparticles," *ACS Photonics*, vol. 4, pp. 2242–2249, 2017.

[70] Y. Fang, M. Han, P. Ge, Z. Guo, and Y. Liu, "Photoelectronic mapping of the spin–orbit interaction of intense light fields," *Nat. Photonics*, vol. 15, no. 2, pp. 115–120, 2021.

[71] L. Han, S. Liu, P. Li, Y. Zhang, H. Cheng, and J. Zhao, "Catalystlike effect of orbital angular momentum on the conversion of transverse to three-dimensional spin states within tightly focused radially polarized beams," *Phys. Rev. A*, vol. 97, no. 5, p. 053802, 2018.

[72] M. Li, Y. Cai, S. Yan, Y. Liang, P. Zhang, and B. Yao, "Orbit-induced localized spin angular momentum in strong focusing of optical vectorial vortex beams," *Phys. Rev. A*, vol. 97, no. 5, p. 053842, 2018.

[73] P. Shi, L.-P. Du, and X.-C. Yuan, "Structured spin angular momentum in highly focused cylindrical vector vortex beams for

optical manipulation," *Opt. Express*, vol. 26, no. 8, pp. 23449–23459, 2018.
[74] P. Shi, L.-P. Du, and X.-C. Yuan, "Optical manipulation with electric and magnetic transverse spin through multilayered focused configuration," *Appl. Phys. Express*, vol. 12, pp. 032001:1–5, 2019.
[75] L. P. Du, A. P. Yang, A. V. Zayats, and X. C. Yuan, "Deep-subwavelength features of photonic skyrmions in a confined electromagnetic field with orbital angular momentum," *Nat. Phys.*, vol. 15, pp. 650–654, 2019.
[76] C. C. Li, P. Shi, L.-P. Du, and X.-C. Yuan, "Mapping the near-field spin angular momenta in the structured surface plasmon polariton field," *Nanoscale*, vol. 12, pp. 13674–13679, 2020.
[77] P. Shi, L. Du, and X. Yuan, "Strong spin–orbit interaction of photonic skyrmions at the general optical interface," *Nanophotonics*, vol. 9, no. 15, pp. 4619–4628, 2020.
[78] P. Shi, L. Du, M. Li, and X. Yuan, "Symmetry-protected photonic chiral spin textures by spin-orbit coupling," *Laser Photon. Rev.*, vol. 15, pp. 2000554:1–9, 2021.
[79] X. Lei, A. Yang, P. Shi, et al., *Photonic Spin Lattices: Symmetry Constraints for Skyrmion and Meron Topologies*, 2021, arXiv: 2103.15366.
[80] Y. Dai, Z. Zhou, A. Ghosh, et al., *Ultrafast Microscopy of a Plasmonic Spin Skyrmion*, 2019, arXiv:1912.03826.
[81] X. Lei, L. Du, X. Yuan, and A. V. Zayats, "Optical spin–orbit coupling in the presence of magnetization: photonic skyrmion interaction with magnetic domains," *Nanophotonics*, 2021. https://doi.org/10.1515/nanoph-2021-0201.
[82] M. Lin, W. Zhang, C. Liu, L. Du, and X. Yuan, "Photonic spin Skyrmion with dynamic position control," *ACS Photonics*, vol. 8, pp. 2567–2572, 2021.
[83] K. Y. Bliokh, F. J. Rodríguez-Fortuño, A. Y. Bekshaev, Y. S. Kivshar, and F. Nori, "Electric-current-induced unidirectional propagation of surface plasmon-polaritons," *Opt. Lett.*, vol. 43, pp. 963–966, 2018.
[84] M. Neugebauer, P. Wozniak, A. Bag, G. Leuchs, and P. Banzer, "Polarization-controlled directional scattering for nanoscopic position sensing," *Nat. Commun.*, vol. 7, pp. 11286:1–6, 2016.
[85] L. Wei, A. V. Zayats, and F. J. Rodríguez-Fortuño, "Interferometric evanescent wave excitation of a nanoantenna for ultrasensitive displacement and phase metrology," *Phys. Rev. Lett.*, vol. 121, pp. 193901:1–6, 2018.
[86] X. Zheng, W. Lei, A. J. L. Adam, and H. P. Urbach, "Accurate feeding of nanoantenna by singular optics for nanoscale translational and rotational displacement sensing," *Phys. Rev. Lett.*, vol. 117, pp. 113903:1–5, 2016.
[87] A. Bag, M. Neugebauer, P. Woźniak, G. Leuchs, and P. Banzer, "Transverse Kerker scattering for Angstrom localization of nanoparticles," *Phys. Rev. Lett.*, vol. 121, pp. 193902:1–6, 2018.
[88] A. B. Young, A. C. T. Thijssen, D. M. Beggs, et al., "Polarization engineering in photonic crystal waveguides for spin-photon entanglers," *Phys. Rev. Lett.*, vol. 115, pp. 153901:1–5, 2015.
[89] J. Petersen, J. Volz, and A. Rauschenbeutel, "Chiral nanophotonic waveguide interface based on spin-orbit interaction of light," *Science*, vol. 346, no. 6205, pp. 67–71, 2014.
[90] Y. Lefier and T. Grosjean, "Unidirectional sub-diffraction waveguiding based on optical spin-orbit coupling in subwavelength plasmonic waveguides," *Opt. Lett.*, vol. 40, no. 12, pp. 2890–2893, 2015.
[91] P. Lodahl, S. Mahmoodian, S. Stobbe, et al., "Chiral quantum optics," *Nature*, vol. 541, pp. 473–480, 2017.
[92] I. Söllner, S. Mahmoodian, S. L. Hansen, et al., "Deterministic photon-emitter coupling in chiral photonic circuits," *Nat. Nanotechnol.*, vol. 10, pp. 775–778, 2015.
[93] B. le Feber, N. Rotenberg, and L. Kuipers, "Nanophotonic control of circular dipole emission," *Nat. Commun.*, vol. 6, pp. 6695:1–6, 2015.
[94] E. Hendry, R. V. Mikhaylovskiy, L. D. Barron, M. Kadodwala, and T. J. Davis, "Chiral electromagnetic fields generated by arrays of nanoslits," *Nano Lett.*, vol. 12, pp. 3640–3644, 2012.
[95] M. Antognozzi, C. R. Bermingham, R. L. Harniman, et al., "Direct measurements of the extraordinary optical momentum and transverse spin-dependent force using a nano-cantilever," *Nat. Phys.*, vol. 12, pp. 731–735, 2016.
[96] H. He, M. E. J. Friese, N. R. Heckenberg, and H. Rubinsztein-Dunlop, "Direct observation of transfer of angular-momentum to absorptive particles from a laser beam with a phase singularity," *Phys. Rev. Lett.*, vol. 75, pp. 826–829, 1995.
[97] M. Li, S. Yan, Y. Liang, P. Zhang, and B. Yao, "Transverse spinning of particles in highly focused vector vortex beams," *Phys. Rev. A*, vol. 95, no. 5, pp. 053802:1–6, 2017.
[98] A. Canaguier-Durand and C. Genet, "Transverse spinning of a sphere in plasmonic field," *Phys. Rev. A*, vol. 89, pp. 033841: 1–10, 2014.
[99] Z. Shao, J. Zhu, Y. Chen, Y. Zhang, and S. Yu, "Spin-orbit interaction of light induced by transverse spin angular momentum engineering," *Nat. Commun.*, vol. 9, pp. 926:1–11, 2018.
[100] M. V. Berry, "Optical currents," *J. Opt. Pure Appl. Opt.*, vol. 11, no. 9, pp. 094001:1–12, 2009.
[101] S. M. Barnett, "Optical Dirac equation," *New J. Phys.*, vol. 16, pp. 093008:1–25, 2014.
[102] I. Bialynicki-Birula, "V photon wave function," *Prog. Opt.*, vol. 36, pp. 245–294, 1996.
[103] I. Bialynicki-Birula, "On the wave function of the photon," *Acta Phys. Pol., A*, vol. 86, pp. 97–116, 1994.
[104] S. A. R. Horsley, "Topology and the optical Dirac equation," *Phys. Rev. A*, vol. 98, pp. 043837:1–13, 2018.
[105] S. M. Barnett, L. Allen, P. RobertCameron, et al., "On the natures of the spin and orbital parts of optical angular momentum," *J. Opt.*, vol. 18, pp. 064004:1–11, 2016.
[106] S. M. Barnett, "Optical angular-momentum flux," *J. Opt. B: Quantum Semiclassical Opt.*, vol. 4, pp. S7–S16, 2002.
[107] I. Bialynicki-Birula and Z. Bialynicka-Birula, "The role of the Riemann–Silberstein vector in classical and quantum theories of electromagnetism," *J. Phys. Math. Theor.*, vol. 46, pp. 053001:1–32, 2013.
[108] I. Bialynicki-Birula and Z. Bialynicka-Birula, "Quantum-mechanical description of optical beams," *J. Opt.*, vol. 19, pp. 125201:1–8, 2017.
[109] F. Tamburini and D. Vicino, "Photon wave function: a covariant formulation and equivalence with QED," *Phys. Rev. A*, vol. 78, pp. 052116:1–5, 2008.
[110] K. Y. Bliokh, A. Y. Bekshaev, and F. Nori, "Optical momentum, spin, and angular momentum in dispersive media," *Phys. Rev. Lett.*, vol. 119, pp. 073901:1–6, 2017.
[111] F. Alpeggiani, K. Y. Bliokh, F. Nori, and L. Kuipers, "Electromagnetic helicity in complex media," *Phys. Rev. Lett.*, vol. 120, pp. 243605:1–6, 2018.

[112] M. F. Picardi, K. Y. Bliokh, F. J. Rodríguez-Fortuño, F. Alpeggiani, and F. Nori, "Angular momenta, helicity, and other properties of dielectric-fiber and metallic-wire modes," *Optica*, vol. 5, pp. 1016–1026, 2018.
[113] L. D. Landau, E. M. Lifshitz, and L. P. Pitaevskii, *Electrodynamics of Continuous Media*, New York, Pergamon, 1984.
[114] K. Y. Bliokh, A. Y. Bekshaev, and F. Nori, "Dual electromagnetism: helicity, spin, momentum, and angular momentum," *New J. Phys.*, vol. 15, pp. 033026:1–30, 2013.
[115] K. Y. Bliokh, M. A. Alonso, E. A. Ostrovskaya, and A. Aiello, "Angular momenta and spin-orbit interaction of nonparaxial light in free space," *Phys. Rev. A*, vol. 82, no. 6, pp. 063825:1–7, 2010.
[116] D. A. Smirnova, V. M. Travin, K. Y. Bliokh, and F. Nori, "Relativistic spin-orbit interactions of photons and electrons," *Phys. Rev. A*, vol. 97, pp. 043840:1–8, 2018.
[117] M. Li, P. Shi, L. Du, and X. Yuan, "Electronic Maxwell's equations," *New J. Phys.*, vol. 22, pp. 113019:1–8, 2020.
[118] M. Elbistan, P. A. Horváthy, and P.-M. Zhang, "Duality and helicity: the photon wave function approach," *Phys. Lett. A*, vol. 381, pp. 2375–2379, 2017.
[119] K. Y. Bliokh, A. Y. Bekshaev, A. G. Kofman, and F. Nori, "Photon trajectories, anomalous velocities, and weak measurements: a classical interpretation," *New J. Phys.*, vol. 15, pp. 073022:1–17, 2013.
[120] M. V. Berry and P. Shukla, "Geometry of 3D monochromatic light: local wavevectors, phases, curl forces, and superoscillations," *J. Opt.*, vol. 21, pp. 064002:1–13, 2019.
[121] A. Aiello and P. Banzer, "The ubiquitous photonic wheel," *J. Opt.*, vol. 18, pp. 085605:1–8, 2016.
[122] M. V. Berry, "Curvature of wave streamlines," *J. Phys. A: Math. Theor.*, vol. 46, pp. 395202:1–6, 2013.
[123] E. Wolf, "A scalar representation of electromagnetic fields: II," *Proc. Phys. Soc.*, vol. 74, pp. 269–280, 1959.
[124] F. J. Belinfante, "On the current and the density of the electric charge, the energy, the linear momentum and the angular momentum of arbitrary fields," *Physica*, vol. 7, pp. 449–474, 1940.
[125] K. Y. Bliokh, J. Dressel, and F. Nori, "Conservation of the spin and orbital angular momenta in electromagnetism," *New J. Phys.*, vol. 16, pp. 093037:1–21, 2014.
[126] R. P. Cameron, S. M. Barnett, and A. M. Yao, "Optical helicity, optical spin, and related quantities in electromagnetic theory," *New J. Phys.*, vol. 14, pp. 053050:1–16, 2012.
[127] S. M. Barnett, R. P. Cameron, and A. M. Yao, "Duplex symmetry and its relation to the conservation of optical helicity," *Phys. Rev. A*, vol. 86, pp. 013845:1–4, 2012.
[128] I. Fernandez-Corbaton, X. Zambrana-Puyalto, and G. Molina-Terriza, "Helicity and angular momentum: a symmetry-based framework for the study of light–matter interactions," *Phys. Rev. A*, vol. 86, pp. 042103:1–14, 2012.
[129] I. Fernandez-Corbaton, X. Zambrana-Puyalto, N. Tischler, X. Vidal, M. L. Juan, and G. Molina-Terriza, "Electromagnetic duality symmetry and helicity conservation for the macroscopic Maxwell's equations," *Phys. Rev. Lett.*, vol. 111, pp. 060401:1–5, 2013.
[130] J. L. Trueba and A. F. Rañada, "The electromagnetic helicity," *Eur. J. Phys.*, vol. 17, pp. 141–144, 1996.
[131] D. L. Andrews and M. M. Coles, "Measures of chirality and angular momentum in the electromagnetic field," *Opt. Lett.*, vol. 37, pp. 3009–3011, 2012.
[132] D. Lipkin, "Existence of a new conservation law in electromagnetic theory," *J. Math. Phys.*, vol. 5, pp. 696–700, 1964.
[133] Y. Tang and A. E. Cohen, "Optical chirality and its interaction with matter," *Phys. Rev. Lett.*, vol. 104, pp. 163901:1–4, 2010.
[134] K. Y. Bliokh and F. Nori, "Characterizing optical chirality," *Phys. Rev. A*, vol. 83, pp. 021803(R):1–3, 2011.
[135] L. D. Landau and E. M. Lifshitz, *Classical Theory of Fields*, 4th ed. Amsterdam, Butterworth-Heinemann, 1994.
[136] D. E. Soper, *Classical Field Theory*, New York, Wiley, 1976.
[137] W. Richard, *Johnson, Handbook of Fluid Dynamics*, 2nd ed. U.S., CRC Press, 2016.
[138] K. Y. Bliokh and F. Nori, "Spin and orbital angular momenta of acoustic beams," *Phys. Rev. B*, vol. 99, pp. 174310:1–9, 2019.
[139] K. Y. Bliokh and F. Nori, "Transverse spin and surface waves in acoustic metamaterials," *Phys. Rev. B*, vol. 99, pp. 020301(R): 1–6, 2019.
[140] D. Leykam, K. Y. Bliokh, and F. Nori, "Edge modes in two-dimensional electromagnetic slab waveguides: analogs of acoustic plasmons," *Phys. Rev. B*, vol. 102, pp. 045129, 2020.
[141] Y. Long, J. Ren, and H. Chen, "Intrinsic spin of elastic waves," *Proc. Natl. Acad. Sci. U.S.A.*, vol. 115, no. 40, pp. 9951–9955, 2018.
[142] K. Y. Bliokh, H. Punzmann, H. Xia, F. Nori, and M. Shats, *Relativistic Field-theory Spin and Momentum in Water Waves*, 2020, arXiv:2009.03245.
[143] S. Golat, E. A. Lim, and F. J. Rodríguez-Fortuño, "Evanescent gravitational waves," *Phys. Rev. D*, vol. 101, pp. 084046:1–13, 2020.
[144] S.-Q. Shen, *Topological Insulators: Dirac Equation in Condensed Matters*, Berlin, Heidelberg, Springer-Verlag, 2012.
[145] M. Z. Hasan and C. L. Kane, "Topological insulators," *Rev. Mod. Phys.*, vol. 82, pp. 3045–3067, 2010.
[146] X.-L. Qi and S.-C. Zhang, "Topological insulators and superconductors," *Rev. Mod. Phys.*, vol. 83, pp. 1057–1110, 2011.
[147] T. Ozawa, H. M. Price, A. Amo, et al., "Topological photonics," *Rev. Mod. Phys.*, vol. 91, pp. 015006:1–76, 2019.
[148] F. D. M. Haldane and S. Raghu, "Possible realization of directional optical waveguides in photonic crystals with broken time-reversal symmetry," *Phys. Rev. Lett.*, vol. 100, pp. 013904: 1–4, 2008.
[149] Z. Wang, Y. Chong, J. D. Joannopoulos, and M. Soljačić, "Observation of unidirectional backscattering-immune topological electromagnetic states," *Nature*, vol. 461, pp. 772–775, 2009.
[150] K. Y. Bliokh, D. Leykam, M. Lein, and F. Nori, "Topological non-Hermitian origin of surface Maxwell waves," *Nat. Commun.*, vol. 10, no. 580, pp. 1–7, 2019.
[151] Q. Zhang, Z. Xie, L. Du, P. Shi, and X. Yuan, "Bloch-type photonic skyrmions in optical chiral multilayers," *Phys. Rev. Res.*, vol. 3, pp. 023109:1–10, 2021.
[152] T. V. Mechelen and Z. Jacob, "Photonic Dirac monopoles and skyrmions: spin-1 quantization," *Opt. Mater. Express*, vol. 9, pp. 95–111, 2019.

[153] S. Tsesses, K. Cohen, E. Ostrovsky, B. Gjonaj, and G. Bartal, "Spin-orbit interaction of light in plasmonic lattices," *Nano Lett.*, vol. 19, pp. 4010–4016, 2019.
[154] S. Tsesses, E. Ostrovsky, K. Cohen, B. Gjonaj, N. H. Lindner, and G. Bartal, "Optical skyrmion lattice in evanescent electromagnetic fields," *Science*, vol. 361, pp. 993–996, 2018.
[155] T. J. Davis, D. Janoschka, P. Dreher, B. Frank, F. J. Meyer zu Heringdorf, and H. Giessen, "Ultrafast vector imaging of plasmonic Skyrmion dynamics with deep subwavelength resolution," *Science*, vol. 368, nos 1–6, p. eaba6415, 2020.
[156] Y. Dai, Z. Zhou, A. Ghosh, et al., "Plasmonic topological quasiparticle on the nanometre and femtosecond scales," *Nature*, vol. 588, pp. 616–619, 2020.
[157] S. Gao, F. C. Speirits, F. Castellucci, S. Franke-Arnold, and S. M. Barnett, "Paraxial skyrmionic beams," *Phys. Rev. A*, vol. 102, pp. 053513:1–6, 2019.
[158] C. Guo, M. Xiao, Y. Guo, L. Yuan, and S. Fan, "Meron spin textures in momentum space," *Phys. Rev. Lett.*, vol. 124, pp. 106103:1–6, 2020.
[159] M. Gilles, P.-Y. Bony, J. Garnier, A. Picozzi, M. Guasoni, and J. Fatome, "Polarization domain walls in optical fibres as topological bits for data transmission," *Nat. Photonics*, vol. 11, pp. 102–107, 2017.
[160] M. V. Berry and M. R. Dennis, "Polarization singularities in isotropic random vector waves," *Proc. R. Soc. A*, vol. 457, pp. 141–155, 2001.
[161] M. V. Berry, "Quantal phase factors accompanying adiabatic changes," *Proc. R. Soc. A*, vol. 392, pp. 45–57, 1984.
[162] D. Leykam, K. Y. Bliokh, C. Huang, Y. D. Chong, and F. Nori, "Edge modes, degeneracies, and topological numbers in non-Hermitian systems," *Phys. Rev. Lett.*, vol. 118, p. 040401, 2017.
[163] T. Bauer, S. Orlov, U. Peschel, P. Banzer, and G. Leuchs, "Nanointerferometric amplitude and phase reconstruction of tightly focused vector beams," *Nat. Photonics*, vol. 8, pp. 23–27, 2013.
[164] A.-P. Yang, F.-F. Meng, P. Shi, L.-P. Du, and X.-C. Yuan, "Mapping the weak plasmonic transverse field by a dielectric-nanoparticle-on-film structure with ultra-high precision," *Opt. Express*, vol. 27, no. 13, pp. 18980–18987, 2019.
[165] F. Meng, A. Yang, P. Shi, L. Du, and X. Yuan, "Mapping the near-field distribution of magnetic fields using a silicon nanoparticle at optical frequencies," *J. Phys. D: Appl. Phys.*, vol. 52, pp. 355002:1–6, 2019.
[166] X. Yin, P. Shi, L. Du, and X. Yuan, "Spin-resolved near-field scanning optical microscopy for mapping of the spin angular momentum distribution of focused beams," *Appl. Phys. Lett.*, vol. 116, pp. 241107:1–4, 2020.
[167] X. Yin, P. Shi, A. Yang, L. Du, and X. Yuan, "Surface plasmon coupled nano-probe for near field scanning optical microscopy," *Opt. Express*, vol. 28, no. 10, pp. 14831–14838, 2020.